Research Article

Crystal structure and docking studies of hexahydrocycloocta[b]pyridine-3-carbonitriles

R. Vishnupriya[1], A.V.K.M. Kowsalyadevi[1], J. Suresh[1], S.Maharani[2], R. Ranjith Kumar[2]

[1]Department of Physics, The Madura College (Autonomous), Madurai, India
[2]Department of Organic Chemistry, School of Chemistry, Madurai Kamaraj University, Madurai, India

Received on April 3, 2014; Accepted on May 18, 2014; Published on June 30, 2014

Correspondence should be addressed to Janakiraman Suresh; e-mail: ambujasureshj@yahoo.com

Abstract

The crystal structures of two new isomorphous pyridine structures, 2-ethoxy-4-(2-flurophenyl)-5,6,7,8,9,10-hexahydrocycloocta[b]pyridine-3-carbonitrile (Ia) and 2-methoxy-4-(4-isopropylphenyl)-5,6,7,8,9,10-hexahydrocycloocta[b]pyridine-3-carbonitrile (Ib) were elucidated by single crystal X ray diffraction. Compound (Ia) $C_{20}H_{21}FN_2O$, crystallizes in the monoclinic system, space group $P2_1/n$ with a = 7.0738 (3) Å, b = 17.3519(8) Å, c = 14.4239 (7) Å, b = 91.837 (2)° and Z = 4. The compound **(Ib)**, $C_{22}H_{25}N_2O$, crystallizes in the same crystal system as compound (Ib), space group $P2_1/c$ with a = 9.7123(6) Å, b = 20.6046(9) Å, c = 10.4657(6) Å, b = 117.208 (3)° and Z = 4. The central heterocyclic ring adopts a planar conformation and the cyclooctane ring adopts a twisted boat chair conformation in both (Ia) and (Ib)**.** The synthesized compounds were screened for their anti-tuberculosis activity and were used to identify lead structures through docking studies, by automated docking. This approach was used to determine the orientation of inhibitors bound in the active site with the enzyme N-acetyl-gamma-glutamyl-phosphate reductase that is involved in arginine biosynthesis in *M. tuberculosis* (*Mtb*AGPR). Details of the preparation, crystal structure determination, intra and inter molecular interactions of the compounds and their docking studies are given.

Introduction

Tuberculosis (TB) remains a deadly disease and continues to claim approximately 2 million lives annually. In affected regions, the disease is recognized as serious impediment to economic and social development. The prevalence of TB has been increasing, and presently nearly two billion individuals worldwide have been exposed to the tubercle bacillus. According to World Health Organization (WHO), roughly one-third of the world population is infected with *Mtb* (Granich *et al.* 2003). Multi-drug resistance and the existence of a large reservoir of latently infected people pose a major threat. Moreover, alternate drugs are very much essential, in addition to the first line drugs normally used to treat TB infection because of the inefficacy of the latter in multi-drug resistant (MDR-TB) and extensive drug-resistant strains (XDR-TB). Also, the treatment regimen for XDR-TB infection usually takes two years.

Pyridine compounds, by large, reveal good anti-mycobacterial activities. Compounds (Ia) and (Ib), belong to the 2-pyridine class of compounds, which show a wide spectrum of biological activities (Perez-Medina *et al*. 1947). It has been reported that the isonicotinic acid (INA) analog of nicotinamide adenine diphosphate (NAD) acts by disturbing the normal cellular metabolism, probably due to its inability to participate in redox reactions. This metabolic disturbance by isoniazid (INH) or INA apparently leads to the breakdown of mycolic acid synthesis and damage to the cell wall structure, as evidenced by the loss of ‘‘acid-fastness’’ of mycobacteria carboxylate anions by enzymatic hydrolysis (Goldman 1954, Kaplan *et al.* 1956, Winder *et al.* 1969). New 1,4-dihydropyridines bearing lipophilic groups in the ring were synthesized

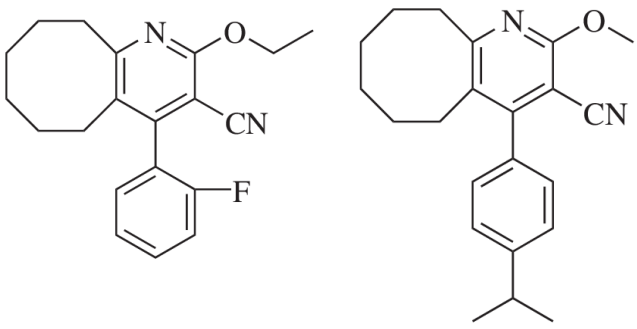

Figure 1. Chemical diagram of the molecule (Ia) (left) and (Ib) (right).

Table 1. The crystal data, experimental conditions and structure refinement parameters of the compound (Ia) and (Ib).

Empirical formula	**$C_{20}H_{21}FN_2O$,**	**$C_{22}H_{25}N_2O$**
Formula weight	324.4	334.5
Temperature	293(2) K	293(2) K
Wavelength	0.71073 Å	0.71073 Å
Crystal system, space group	$P2_1/n$, Monoclinic	P $2_1/c$, monoclinic
Unit cell dimensions	a = 7.0738(3)Å, b=17.3519(8)Å c = 14.4239(7)Å, β=91.837(2)°	a = 9.7123(6)Å, b =20.6046(12) Å, c = 10.4657(6)Å, β=117.208(3)°
Volume	1769.54 (2) $Å^3$	1862.64(3) A^3
Z, Calculated density	4, 1.22 mg/m^3	4, 1.19 mg/m^3
Absorption coefficient	0.083 mm^{-1}	0.073 mm^{-1}
F(000)	688	720
Crystal size	0.19x0.16x0.14mm^3	0.17x0.14x0.11mm^3
Theta range for data collection	2.3 to 26.1 deg	2 to 28.3 deg
Limiting indices	-8<=h<=8, -21,=k<=21, -17<=l<=17	-12<=h<12, -27<=k<18, -13<=l<=13
Reflections collected / unique	16997 / 3516 [R(int) = 0.0308]	16998 / 4594[R_{int} = 0.0219]
Completeness to theta	99.8 %	99.4%
Absorption correction	ω -scan	ω -scan
Refinement method	Full-matrix least-squares on F^2	Full-matrix least-squares on F^2
Data / restraints / parameters	3516 / 173 / 283	4594/ 3/ 251
Goodness-of-fit on F^2	1.036	1.036
Final R indices [I>2sigma(I)]	R_1 = 0.0489, wR_2 = 0.1311	R_1 = 0.0610, wR_2 = 0.160
R indices (all data)	R_1 = 0.0769, wR_2 = 0.1503	R_1 = 0.085, wR_2 = 0.178
Largest diff. peak and hole	0.185 and -0.197 eA^{-3}	0.501 and -0.335 $eÅ^{-3}$

and evaluated for anti-tuberculosis activity upon the assumption that these compounds could act as pro-drugs, and after penetration into the cell wall, would be converted into the 3,5-carboxylate anions by enzymatic hydrolysis (Desai *et al.* 2001). *N*-Alkyl-1,2-dihydro -2-thioxo-3-pyridinecarbothioamides 2.18. *N*-Pyridinylsalicylamides have been identified as a novel pyridine class of compounds with anti-tuberculosis activity (Ubiali *et al.* 2002). In the course of screening for the discovery of new compounds that could be useful for the treatment of TB, we report the synthesis and single crystal X-ray studies of two novel spiro compounds, (Ia) and (Ib) (Figure 1), together with docking studies.

Synthesis

Preparation of compound (Ia)

A mixture of cyclooctanone (1 mmol), 2- fluro benzaldehyde (1 mmol) and malononitrile (1mmol) were taken in ethanol (10 mL) to which lithium ethoxide (1 equiv) was added. The reaction mixture was heated under reflux for 2–3 h. After completion of the reaction (TLC), the reaction mixture was poured into crushed ice and extracted with ethyl acetate. The excess solvent was removed under vacuum and the residue was subjected to column chromatography using a petroleum ether/ethyl acetate mixture (95:5 v/v) as eluent to obtain the pure product. The melting point was 99–101°C and yield 66%.

Preparation of compound (Ib)

A mixture of cyclooctanone (1 mmol), 4-isopropyl benzaldehyde (1 mmol) and malononitrile (1mmol) were taken in methanol (10 mL) to which lithium ethoxide (1 equiv) was added. The reaction mixture was heated under reflux for 2–3 h. After completion of the reaction (TLC), the reaction mixture was poured into crushed ice and extracted with ethyl acetate. The excess solvent was removed under vacuum and the residue was subjected to column chromatography using a petroleum ether/ethyl acetate mixture (95:5 v/v) as eluent to obtain the pure product. The melting point was 160–161°C and yield 75%.

Structure Determination and Refinement

Intensity data of the single crystal of the compounds were collected using a Bruker AXS Kappa APEX II single crystal CCD Diffractometer equipped with graphite-monochromated MoKα radiation (λ=0.71073Å) at room temperature. Accurate unit cell parameters were determined from the reflections of 36 frames measured in three different crystallographic zones. The data collection, data reduction and absorption correction were performed by APEX2, SAINT-Plus and SADABS (Bruker 2004). The structure was solved by the direct method procedure and the non-hydrogen atoms were subjected to anisotropic refinement by full-matrix least squares on F^2 using SHELXL -97 (Sheldrick 2008). Molecular graphics were drawn using PLATON (Spek 2009). The hydrogen atoms were placed in calculated positions and included in the refinement using the riding model with C—H = 0.93–0.98 Å and U_{iso} = 1.2*U*eq(C,N) for the CH and CH_2 groups and U_{iso} = 1.5*U*eq(C) for the CH_3 group. The crystal data, experimental conditions and structure refinement parameters for the compounds (Ia) and (Ib) are presented in Table 1. Their molecular structures, showing the atom numbering scheme using ORTEP 3 (Farrugia 1997) are shown in Figure 2. The disordered model was refined using the tools available in SHELXL-97 (Sheldrick 2008) and SADI for restraining distances. A combination of *SIMU* (similar *Uij* parameters) and *DELU* (rigid bonds) restraints were applied (Sheldrick 2008). Also, a DFIX restraint was used to stabilize the refinement of the disordered atoms.

Docking Studies

Docking studies were carried out for the reported compound with an enzyme involving arginine biosynthesis in *Mtb*. Arginine biosynthesis has been shown to be essential in Mtb. An ArgF mutant requiring exogenous L-arginine for growth *in vitro* has shown reduced virulence in immunodeficient SCID mice and is highly attenuated in immune competent mice, suggesting that L-arginine availability is restricted *in vivo* (Gordhan *et al.* 2002). A recent study has identified ArgA, an essential enzyme that catalyzes the conversion of L-glutamate to a-N-acetyl-L-glutamate, as the initial step in L-arginine biosynthesis (Errey *et al.* 2005). To begin with, high resolution of 1.8Å X-ray crystal structures of enzymes involved in arginine biosynthesis from *Mtb* were searched in the protein data bank (PDB).

The search analysis showed that the X-ray crystal structure of N-acetyl-g-glutamyl phosphate reductase from *Mtb* (*Mtb*AGPR; PDB ID 2I3G) was identified as the suitable candidate for the docking studies. The corresponding coordinates of *Mtb*AGPR were then retrieved from RCSB PDB. Moreover, for docking studies, only protein atoms were considered. The water oxygen atoms and other ligand atoms present in the PDB file were removed using pyMOL (Delano 1998). It was solvated in a rectangular box of 14,410 water molecules using the "SPC216" model system in order to mimic the physiological behavior of the molecules. The energy of the solvated model was minimized without restraints for 1000 steps using the steepest descent algorithm which is followed by 1000 steps of conjugate gradient algorithm. To minimize the ligand's energy for docking, MMFF94 force field with conjugate gradient algorithm was carried out in the OpenBabel platform of PyRx (Wolf 2009). The active site pocket of *Mtb*AGPR was identified using online server Computed Atlas of Surface Topography (CASTp). Subsequently, the synthesized compound was docked at the active site identified by CASTp.

Molecular docking of the compound with the protein molecule was carried out using the program

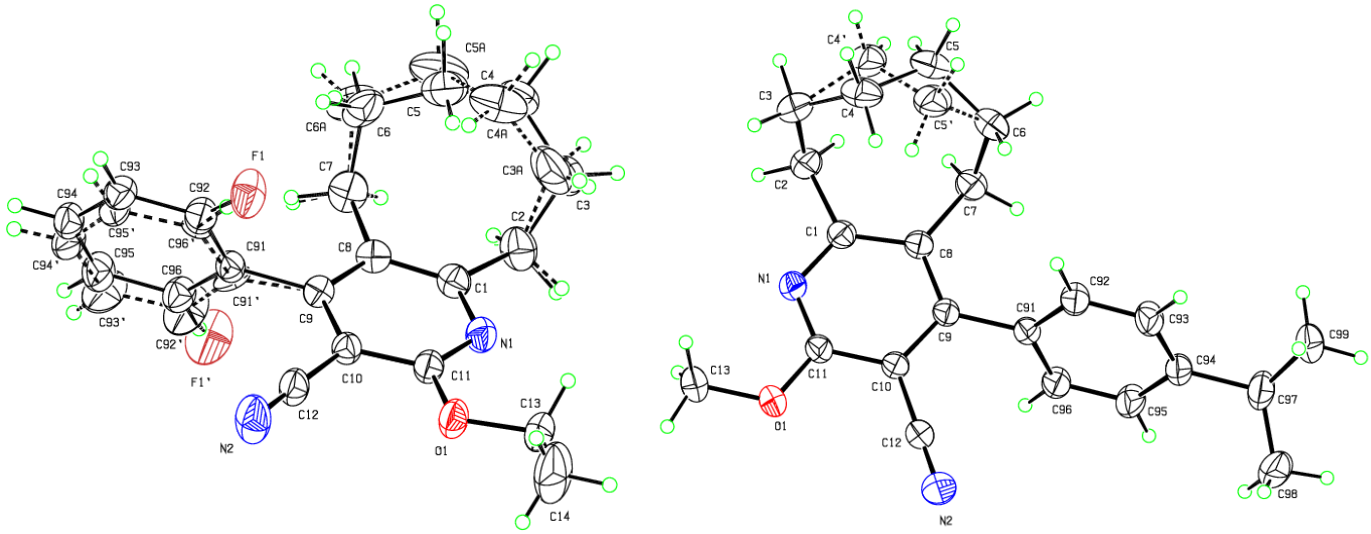

Figure 2. The molecular structure of compound (**Ia)** (left) and (**Ib)** (right), showing the atom numbering scheme. Displacement ellipsoids are drawn at 30% probability level, using ORTEP 3. Hydrogen atoms are drawn as spheres of arbitrary size.

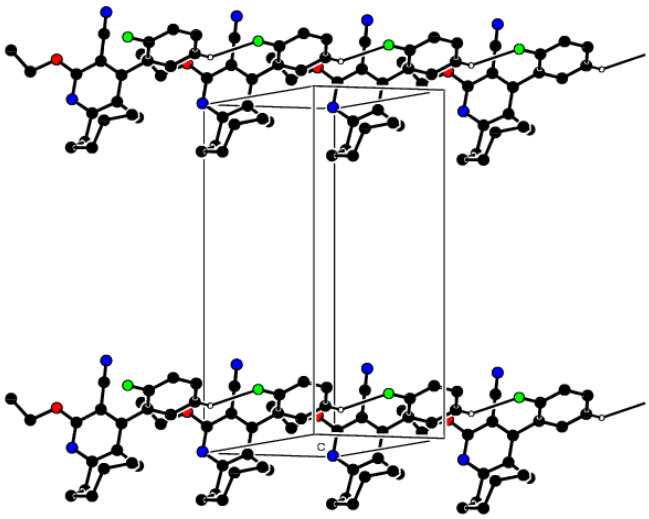

Figure 3. Linear chain motif $C_1^1(6)$ of compound (Ia).

AutoDoCK4v2 (Goodsell 1998). A grid box of 76 x 62 x 84 with the grid spacing of 0.375 Å was chosen. The grid was automatically centered at the middle of the active site. The electrostatic and atomic interaction maps for all atom types of the ligand molecule were calculated using the *autogrid* module of the AutoDock program. The Lamarckian genetic algorithm (LGA) was employed up to 100 runs for docking studies. The values and other parameters were taken as defaults in the docking program. The conformation of the docked ligand molecule was analyzed based on the binding energy values.

The biological activity studies of the compounds (Ia) and (Ib) are presently in progress. Apart from screening these compounds against MTB, their activity against antimicrobial and antifungal activities are also being done.

Results and Discussion

The molecular structures of (Ia) and (Ib) are shown in Figure 1. The cyclooctane ring in the two compounds adopts a twist boat chair conformation, as found in other related structures (Xiong *et al.* 2007, Fun *et al.* 2010, Suresh *et al.* 2007). The central pyridine component of (Ia) and (Ib) are effectively planar, with a maximum deviation from the mean plane that of -0.0132 (4) Å for atom C10 of (Ia) and 0.0064 (1) Å for atom C8 of compound (Ib). This slight deviation may be associated with the presence of three adjacent substituents, at atoms C9 - C11. The deviation of the nitrile atoms (C12, N2) from the mean plane of the pyridine ring system (N1, C1, C8 - C11) is -0.0338 (6) Å and -0.0622 (5) Å in compound (Ia), 0.0491 (8) Å and 0.1179 (7) Å in compound (Ib).

The C4, C5 carbon atoms with their corresponding hydrogen atoms of the cyclooctane ring and the fluoro-substituted benzene ring of compound (Ia) are statistically disordered over two conformations with a site-occupancy ratio of 0.554(8) : 0.446(8) (9) and 0.793 (2) : 0.207 (2), respectively. The C4, C5 carbon atoms with their corresponding hydrogen atoms of cyclooctane ring of compound (Ib) are disordered with occupancy factors of 0.2242 (1) : 0.70379 (1), respectively.

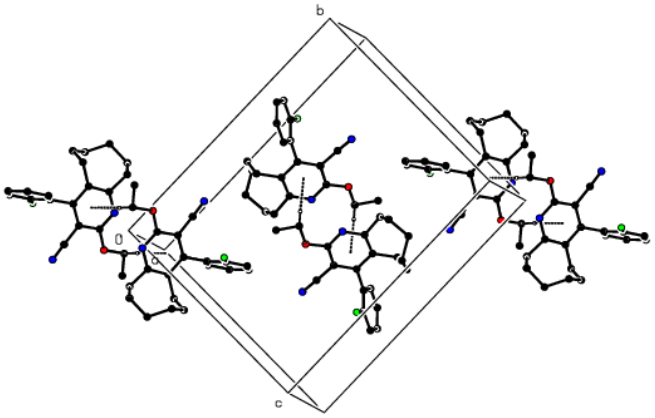

Figure 4. A pair of inversely related molecules are interconnected through C-H…π interaction of compound (Ia).

The triple-bond character of the C12 ≡ N2 bond is 1.136 (3) Å and 1.138 (3) Å in compounds (Ia) and (Ib), respectively; this is similar to the other related structures (Ramesh *et al.* 2009a, b) and the C10-C12 ≡ N2 bond angle of 178.64(1)° and 178.40(1)°, defining the linearity of the cyano group are typical of this group of 2-oxopyridine-3-carbonitrile compounds (Black *et al.* 1992, Hussain *et al.* 1996). The carbonitrile group lies almost in the plane of the attached planar pyridine ring system (N1, C1, C8-C11). The torsion angles (C9-C10-C12-N2) and (C11-C10-C12-N2) define the orientation of the carbonitrile group with the pyridine ring (-152.59(6)° and 99.21(2)° in compounds (Ia) and (Ib) respectively and -28.30(6)° and -78.81 (2)° in compounds (Ia) and (Ib) respectively).

The bond distances in the central pyridine ring (C1/C8-C11/N1) range from 1.315(1) - 1.398 (2) Å in compound (Ia) and 1.313(1) - 1.401(2) Å in compound (Ib), suggesting possible resonance delocalization of the π electrons over the ring (Allen *et al.* 1987). The phenyl rings of the molecules are planar. Steric hindrances rotate the phenyl ring out of the plane of the central pyridine ring by 75.23 (8)° and 73.67 (1)° in compound (Ia) and (Ib), respectively. These values are different from those in similar structures (Patel *et al.* 2002a, Bolte 1998).

The phenyl substituent at C9 of the pyridine ring has a (-) anticlinal conformation in compound (Ia) and (+) synclinal conformation in compound (Ib), which is evidenced by the C96-C91-C9-C10 torsion angles -106.47(1) and 72.27(1)° in (Ia) and (Ib), respectively. The ethoxy group in compounds (Ia) is coplanar with the heterocyclic ring plane which is evidenced by the torsion angle C11-O1-C13-C14 = 165.43 (2)° in (Ia). There is a long Csp^2-Csp^1 which is evidenced by the C10-C12 bond which is 1.425(2)Å and 1.436(2) Å in compounds (Ia) and (Ib), respective-

ly. This is due to conjugation which has the similar orientation in similar related structures (Ramesh *et al.* 2009a, b).

Crystal Packing

Both the structures differ in the nature of the substituents at the 2-position of the central pyridine ring and on the pendant aryl ring. This simple change in the structure substantially alters the intermolecular interaction patterns.

In the crystal structure of the compound (Ia), the C95 atom of the aryl ring is involved in the intermolecular interaction C95—H95···F1$^{(i)}$ with the F1 atom forming a chain $C_1^1(6)$ motif (Bernstein *et al.* 1995) around inversion centers of the unit cell. These motifs form a linear infinite double chain running along the a-axis as shown in Figure 3 [symmetry code: (i) 1+x, y, z]. In addition, the adjacent molecules are linked together by a C—H…$\pi^{(ii)}$ □ interaction forming a inversely related dimer (Figure 4) [symmetry code: (ii) -x,-y,-z].

The crystal structure of the compound (Ib) contains a π···π interaction, Cg1···Cg1^{i} (Cg1 is the centroid of the pyridine ring), with Cg1···Cg1^{i} separation of 3.7625 (2) Å [symmetry code: (i) 1-x, -y, 1-z] as shown in Figure 5. Neither C-H…O nor C-H…p interactions are observed between these chains. However, there are several van der Walls interactions between them in both compounds. Inter molecular and intra molecular hydrogen bond geometry of (Ia) is detailed in Table 2.

Docking Analysis

The docking study was performed by automated docking and was used to determine the orientation of the inhibitors bound in the active site of MtbAGPR (PDB code: 2I3G) for antituberculosis**.** The target proteins had four identical chains, namely A, B, C and D, in the PDB file. However, only a monomer was chosen for analysis. Forty seven pockets were predicted using the *Castp* program. Of that, only one pocket was considered .This binding pocket was chosen on the basis of the presence of conserved catalytic residues such as Asp108, Arg114, Tyr211,His217, His219, Glu222, Asp319, Asn320, and Leu321, as well as six glycine residues (numbers 16,19, 157, 192, 249, 324) that have been reported in the literature (Cherney *et al.* 2007). Interestingly, this active site pocket was also the binding pocket for the NADP+ molecule. Thus, the biologically favorable site for docking was chosen.

Table 2. Hydrogen bonds [Å and°] of compound (Ia).

D-H...A	d(D-H)	d(H...A)	d(D...A)	DHA
C(95)-H(95)...F(1)$^{(i)}$	0.93	2.52	3.2859(4)	139
C(13)-H(13B)...Cg1$^{(ii)}$	0.93	2.89	3.8000(3)	157

Symmetry transformations used to generate equivalent atoms:
(i) 1+x, y, z
(ii) -x,-y,-z

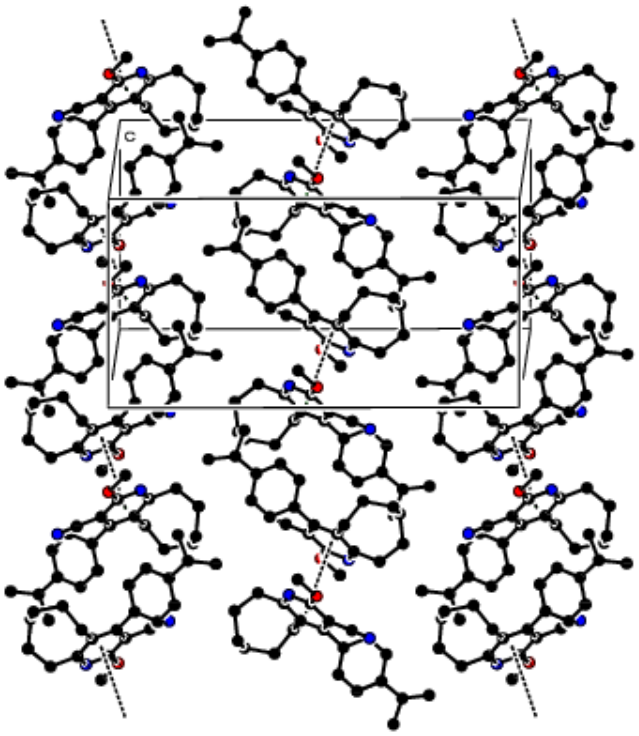

Figure 5. A partial packing view of the compound (Ib) showing a pair of molecules interconnected through a π···π stacking interaction**.**

The docking of ligand molecules with *Mtb*AGPR revealed that both inhibitor compounds exhibited bonding with one or more amino acids (Table 3) in the active pocket as shown in Figure 6. The study also revealed that the bipyridine scaffolds is the key residues at the active site of *Mtb*AGPR. Moreover, both compounds have minimum binding energy hence could be considered as a good inhibitor of *Mtb*AGPR. Between the compounds, (Ib) showed the highest binding energy score (Table 3). The ligands used for the docking studies showed similar modes of binding interactions as that of the complex. Superimposition of the antibiotics within the NADP+ molecule binding pocket indicates that the overlapping binding determinants are possible because of the remarkable correspondence in the overall shape of each antibiotic (Figure 8). These *in silico* results revealed that the synthesized bipyridine compounds may be an effective drug candidate for Mtb.

Conclusion

2-ethoxy-4-(2-flurophenyl)-5,6,7,8,9,10-hexahydrocycloocta[b]pyridine-3-Carbonitrile (Ia) and 2-methoxy-4-(4-

Table 3. The results of both the compounds docked with the enzyme *Mtb*AGPR.

Compound	Hydrogen bond	Distance (Å) D-H…A	B.E (kcal/mol)
Ia	(ARG 212) N-H…O (ARG 218) N-H…O N-H…O(ARG 218)	3.7 2.0 3.4	-8.16
Ib	(ARG 114) N-H…O (ARG 114) N-H…O N-H…O (PRO 89)	2.6 2.5 3.8	-7.55

isopropylphenyl)-5,6,7,8,9,10-hexahydrocycloocta[b] pyridine-3-carbonitrile (Ib) were synthesized. The single crystals of these compounds were obtained by the slow evaporation method with ethyl acetate as the solvent. The structure determination of small molecules were carried out and discussed based on the physicochemical parameters as well as the earlier reports available in the literature. Molecular docking studies were performed with the suitable protein target. In addition, the orientation of the aryl rings can affect the alignment of these rings at a binding site and hence influence bioactivity (Quail *et al.* 2005). From the docking analysis of the two compounds with the receptor of 2I3G, it was found that (Ib) shows better binding with the receptor, as compared to (Ia), with the energy of -7.55 kcal/mol. However, since there is very small change in the binding energy, both compounds can be used for the inhibition of 2I3G.

The theoretical outcome of the docking studies highlighted that the minimum binding energy of the molecules with the target protein may make these newly synthesized bipyridine compounds good inhibitors of *Mtb*AGPR. Therefore it is pleasing to state that the docking studies have widened the scope of the development of bipyridine compounds as promising antituberculosis agents.

Author's Contribution

Authors 1, 2 and 3 involved in the crystal growth, data collection and crystallography work. Authors 4 and 5 involved in the synthesis and NMR spectra. First and second author is the third author's student and fourth author is the fifth author's student.

Conflict of interest

No conflict of interest

Supplementary Material

Crystallogtaphic data (excluding structure factors) for the structures of (Ia) and (Ib) reported in this paper

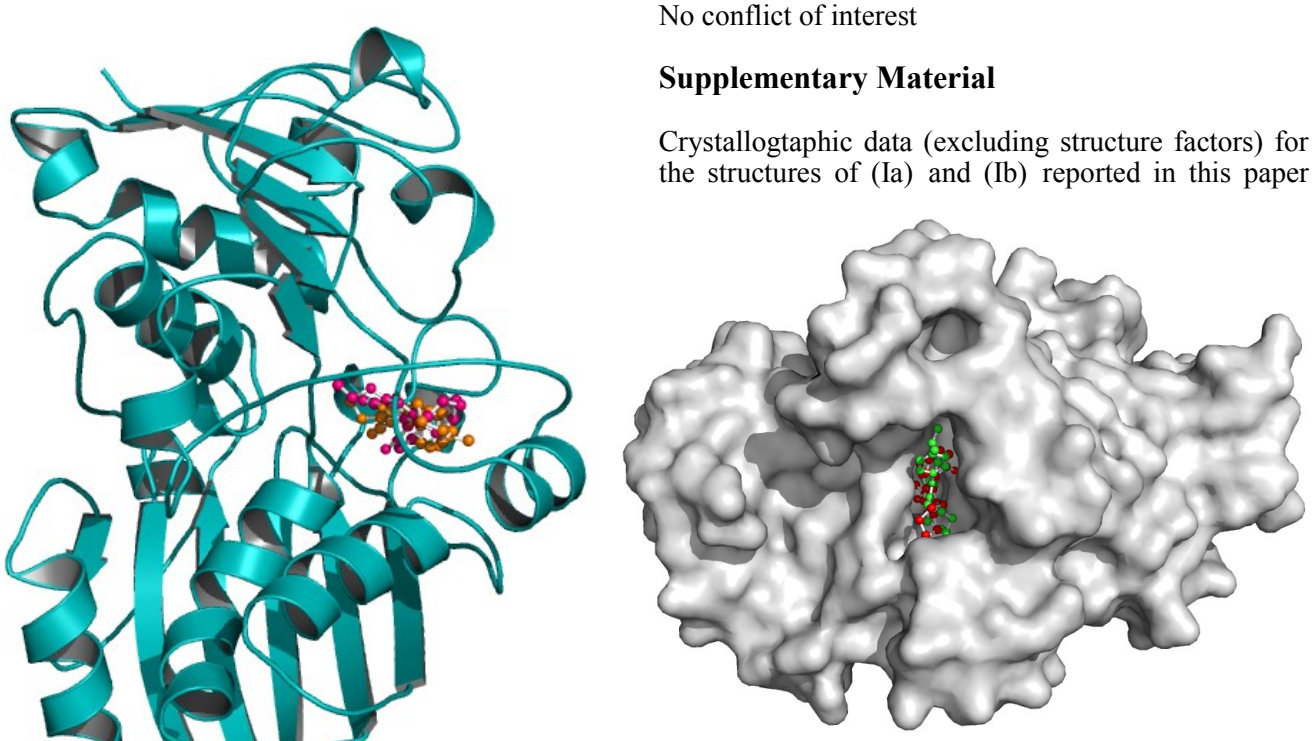

Figure 6. Monomer of *Mtb*AGPR docked with both compounds (left) and surface view of the binding pocket of the bipyridine compounds in *Mtb*AGPR (right).

have been deposited with the Cambridge Crystallographic data Centre as supplementary publication CCDC 994649 & CCDC 994650. Copies of the data can be obtained, free of charge, on application to, CCDC, 12 Union Road, Cambridge, and CB2 1 EZUK; Fax: 044-1223-336033; Email: deposit@ccdc.cam.uk or at: http://www.ccdc.cam.ac.uk/.

Acknowledgements

JS thanks the UGC for the FIST support. JS and RV thank the management of Madura College for their encouragement and support. RRK thanks University Grants Commission, New Delhi, for funds through Major Research Project F. No. 42-242/2013 (SR).

Conflicts of interest

The author has no conflicts of interest.

References

Allen FH 2002 The Cambridge Structural Database: a quarter of a million crystal structures and rising *Acta Cryst* B **58** 380-388

Allen FH, Kennard O, Watson DG, Brammer L, Orpen AG & Taylor R 1987 *J Chem Soc Perkin Trans*. **2** S1–19

Balzani S & Campagna S 2007 Photochemistry and Photophysics of Coordination Compounds I & II (Topics in Current Chemistry), vol. 280-281. Berlin: V. Springer Verlag

Bernstein J, Davis RE, Shimoni L & Chang NL 1995 Patterns in Hydrogen Bonding: Functionality and Graph Set Analysis in Crystals. *Angew Chem Int Ed Engl* **34** 1555-1573

Black SN, Davey R J, Slawin AMZ & Williams DJ 1992 *Acta Cryst* C **48** 323-325

Bolte M 1998 3-Methoxy-2,4,6-triphenylpyridine at 173K *Acta Cryst* C **54** 132-134

Bruker 2004 APEX2 and SAINT. Bruker AXS Inc, Madison, Wisconsin, USA

Cherney LT, Cherney MM, Garen CR, Chunying Niu , Fatemeh Moradian & Michael James NG 2007 Crystal Structure of N-acetyl-g-glutamyl-phosphate Reductase from Mycobacterium tuberculosis in Complex with NADP+ *J Mol Biol* 367 1357 - 1369

DeLano WL 2002 The PyMOL Molecular Graphics System . DeLanoScientific, San Carlos, CA, USA

Desai B , Sureja D , Naliapara Y , Shah A & Saxena AK 2001 Synthesis and QSAR studies of 4-substituted phenyl-2,6-dimethyl-3, 5-bis-N-(substituted phenyl)carbamoyl-1,4-dihydropyridines as potential antitubercular agents. *Bioorg Med Chem* **9** 1993

Errey JC & Blanchard JS 2005 Functional characterization of a novel ArgA from Mycobacterium tuberculosis. *J Bacteriol* **187** 3039-3044

Farrugia LJ 1997 ORTEP-3 for windows-a version of ORTEPIII with a graphical user interface (GUI). *J Appl Cryst* **30** 568

Fun HK, Yeap CS, Ragavan RV, Vijayakumar V & Sarveswari S 2010 4,5,6,7,8,9-Hexahydro-2H-cycloocta[c]pyrazol-1-ium-3-olate *Acta Cryst* E **66** o3019

Goldman DS 1954 On the mechanism of action of isonicotinic acid hydrazide *J Am Chem Soc* **76** 2841

Goodsell DS, Morris GM & Olson AJ 1998 Automated docking of flexible ligands: Applications of autodock. *J Mol Recog* **9** 1-5

Gordhan BG, Smith DA, Alderton H, McAdam RA, Bancroft GJ & Mizrahi V 2002 Construction and phenotypic characterization of an auxotrophic mutant of Mycobacterium tuberculosis defective in L-arginine biosynthesis. *Infect Immun* **70** 3080-3084

Granich R, Wares F, Suvanand S & Chauhan LS 2003 Tuberculosis control in India. *Lancet Infect Dis* **3** 535-536

Hannon MJ & Childs LJ 2006 Helices and Helicates: Beautiful Supramolecular Motifs with Emerging Applications. *Supramol Chem* **16** 7-22

Hussain Z, Fleming FF, Norman RE & Chang SC 1996 *Acta Cryst* C **52** 1010-1012

Kaes C, Katz A & Hosseini MW 2000 Bipyridine: The Most Widely Used Ligand. A Review of Molecules Comprising at Least Two 2,2'- Bipyridine Units. *Chem* **100** 3553-3590

Patel UH, Dave CG, Jotani MM & Shah HC 2002a 1,3-Dimethyl-2-oxo-4,6-diphenyl-1,2,3,4-tetrahydropyridine-3-carbonitrile. *Acta Cryst* C **58** o191-o192

Perez-Medina LA, Merriella RP & McElvain SM 1947 *J Am Chem Soc* **69** 2574-2579

Quail JW, Doroud A, Pati HN, Das U & Dimmock JR 2005 (E,E)-2-(4-Fluorophenylmethylene)-6-(4-Nitrophen-ylmeThylene)Cyclohexanone. *Acta Crystallographica* E **61** o1774-o1776

Ramesh P, Subbiahpandi A, Thirumurugan P, Perumal PT & Ponnuswamy MN 2009 *Acta Cryst* E **65** o450

Ramesh P, Sundaresan SS, Thirumurugan P, Perumal PT & Ponnuswamy MN 2009 *Acta Cryst* E **65** o996-o997

Schalley CA, Lützen A & Albrecht M 2004 Approaching Supramolecular Functionality *Chem Eur J* 10 1072-1080

Sheldrick GM 2008 A short history of *SHELX*. *Acta Cryst* A **64** 112-122

Smith AP, Fraser CL, McCleverty JA & Meyer TJ 2004 Comprehensive Coordination Chemistry II Vol 1. Oxford: Elsevier

Spek AL 2009 Structure validation in chemical crystallography *Acta Cryst* D **65** 148-155

Suresh J, Suresh Kumar R, Perumal S & Natarajan S 2007 1'-Methylcyclooctane-1-spiro-3'-pyrrolidine-2'-spiro-3"-indoline-2,2"-dione and 1,1'-dimethylpiperidine-3-spiro-3'-pyrrolidine-2'-spiro-3"-

indoline-2",4-dione *Acta Cryst* C **63** o538-o542
Ubiali D, Pagani G, Pregnolato M, Piersimoni C, Munoz JP, Gascon AR & Terreni M 2002 New N-alkyl-1, 2-dihydro-2-thioxo-3-pyridine carbothioamides as antituberculous agents with improved pharmacokinetics. *Bioorg Med Chem Lett* **12** 2541
Winder FG & Collins P 1969 The effect of isoniazid on nicotinamide nucleotide concentrations in tubercle bacilli. A correction and further observations. *Am Rev Respir Dis* **100** 101
Wolf LK 2009 Digital Briefs C&EN **87** 31
Xiong Y, Gao WY, Deng KZ, Chen HX & Wang SJ 2007 5,6-dihydroxy- 1,2,3,13- tetramethoxy -6,7-dimethyl- 5,6,7,8 – tetrahydrobenzo [3,4] cycloocta [1,2-f] [1,3] – benzodioxol-5-yl benzoate sesquihydrate *Acta Cryst* E **63** o333-o334